Proc. Natl. Sci. Counc. ROC(A)
Vol. 19, No. 5, 1995. pp 361-370

Numerical Model of Three-Phase Transformer Banks and a Shell-Type Transformer for Calculating the Transient Current

CHING-LIEN HUANG, JIM-CHWEN YEH, CHIN E. LIN, AND CHENG-LONG CHENG

Department of Electrical Engineering
National Cheng Kung University
Tainan, Taiwan, R.O.C

(Received April 20, 1994; Accepted February 17, 1995)

ABSTRACT

Measurements of transient inrush currents in three-phase transformers offer important data for power system operation and protection. Because three-phase transformers are more widely used in industrial applications than are single-phase transformers, the inrush current of the three-phase transformer is worthy of investigation. Therefore, a method for accurately predicting transient inrush currents is useful in system operation and protection. This paper proposes a simple method, extended from single-phase transformers, to investigate three-phase transformer inrush currents Various structures of three-phase transformers, including winding connections and loading conditions, are discussed. The simulation results are compared with experimental results. The proposed method is simple and effective for transformer banks and a shell-type (five-limb) transformer.

Key Words: transient, inrush current analysis, three-phase transformer, simulation and experiment

I. Introduction

Since the structure of three-phase transformers is multiple compared to that of single-phase transformers, the magnetic loop analysis of a three-phase transformer is more complicated and difficult to study. Analysis of the saturation characteristics in three-phase transformers has been a necessary procedure in the study of inrush currents in three-phase transformers in much research and design work. Regarding inrush currents in three-phase transformers, several known methods have been developed (Macfadyen *et al.*, 1973; Nakra and Barton, 1974; Rahman and Gangopadhyay, 1986; Yacamin and Abu Nasser, 1986) to derive an analytical solution or to perform a numerical simulation by applying various techniques. The main drawback to those methods is their mathematical complexity in analysis and procedural difficulty in parameteric data acquisition. Furthermore, because these methods can not accurately cover actual loading conditions, they are not adequate for representing general operating conditions of power systems. Only special cases have been studied.

An improved model (Lin *et al.*, 1993a) to press the single-phase inrush current from a finite difference form using digital data acquisition was developed in our laboratory. This model is simple and accurate in inrush current analysis as well as for other applications for single-phase transformers. Based on a general extension of this model, a new method of inrush current study for three-phase transformers is proposed. The proposed method can also provide effective analytical data via simple modelling with straightforward procedures. Various structures of three-phase transformers, including electrical winding connections using different three-phase structures, are investigated by considering various operating conditions, such as switching-on angle, loading power factors and remanent flux. The simulation results are compared with experiment results with very good agreement.

II. The Proposed Method

1. Analysis of Saturation Characteristics in Transformers

The saturation-characteristics of a transformer must be known to calculate the transformer inrush current by simulation. Many methods to obtain the saturation characteristics of a transformer have been described in the technical literature (Badawy and Youssef, 1983; Keyhani and Miri, 1988; Prusty and Rao, 1984; Rivas *et al.*, 1981; Swift, 1971). Defects may be found in these methods either in their compli-

cated procedures or in the precision of measurements from field test data. A method using a polynomial form to determine transformer saturation characteristics without field test data (Lin *et al.*, 1989) was developed in our laboratory. This method formulates a simple but accurate saturation representation using PC-AT real time data acquisition. It does not require field test data to represent the saturation curve. Based on this technique, the transformer saturation characteristics can be obtained for further study (Lin *et al.*, 1993a, 1993b).

In a single-phase transformer, calculation of the inrush current is simple due to the independent magnetic circuit; in a three-phase transformer, this calculation becomes much more complicated due to the interaction of the magnetic circuits. For different types of three-phase transformers, such as transformer banks and five-limb transformers, there are different mechanical structures and magnetic circuits. In addition, electrical connections, including delta-wye and delta-delta, strongly influence the saturation characteristics. The saturation characteristics of three-phase transformers will be further described below:

A. Transformer Banks

(1) For delta-wye connection:

A transformer bank is essentially three separate single-phase transformers. The magnetic circuit of the iron core in each phase of the transformer is independent. Figure 1 shows the hysteresis loop in phase A at 110V when three-phase power is supplied to a three-phase transformer bank of a delta-wye connection. Figure 1 also shows the hysteresis loop in phase A at 110V when a single-phase power source is supplied only to a independent phase A. The other phases display the same behavior. This proves that delta-wye connected transformer banks can be treated as single-phase transformers.

(2) For delta-delta connection:

Figure 2 shows a hysteresis loop in phase A at 110V when a delta-delta connected transformer bank is energized by a three-phase power source. Comparing Fig. 2 with Fig. 1, obviously, the peak value of the magnetizing current with the delta-delta connection is smaller than that with the delta-wye connection. A delta-delta connected transformer also has a circular current due to the unbalanced three-phase secondary load. The circular current diminishes the main flux and reduces the chance of iron core saturation. The peak value of the magnetizing current in the saturated region becomes smaller and results in a smaller inrush current as will be described in a later section.

B. Five-Limb Transformers

Different types of three-phase transformer core structures are shown in Fig. 3. The mechanical structures of three-phase transformers have essentially evolved from three single-phase transformers connected by a common limb, as in Fig. 3(b). When a three-phase circuit is balanced, the net flux of the common limb is zero. Alternatively, when the common limb is replaced by two edge limbs, a five-limb three-phase transformer in Fig. 3(c) is formed. (Typing Fig. 3)

(1) For delta-wye connection:

The magnetic circuit in each phase of the five-limb transformer in Fig. 3(c) can approximately be considered as independent. The flux interaction between the phases is not significant. The peak magne-

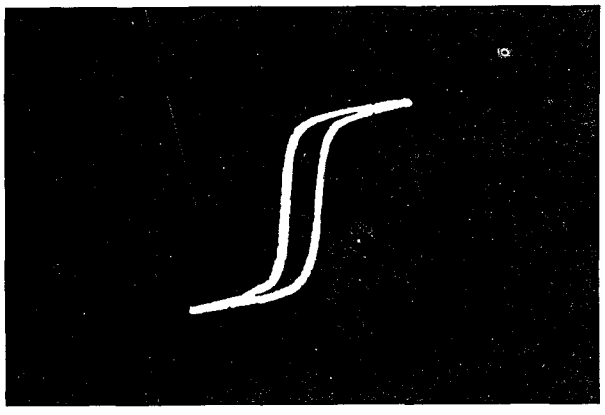

Fig. 1. Hysteresis loop of phase A in (a) delta-wye connected three-phase transformer banks, measured at three-phase voltage 110V, and (b) three-phase transformer banks, measured independently at single-phase voltage 110V.

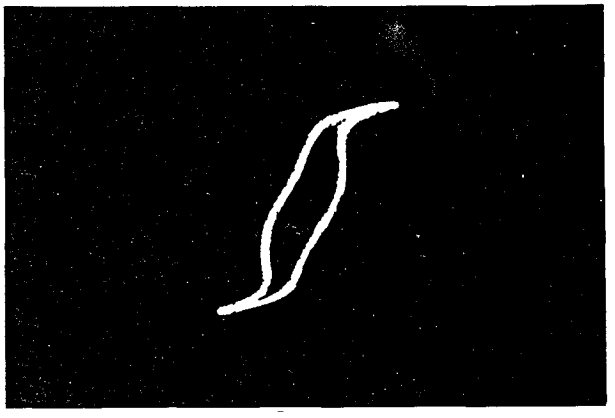

Fig. 2. Hysteresis loop of phase A in delta-delta connected three-phase transformer banks measured at three-phase voltage 110V.

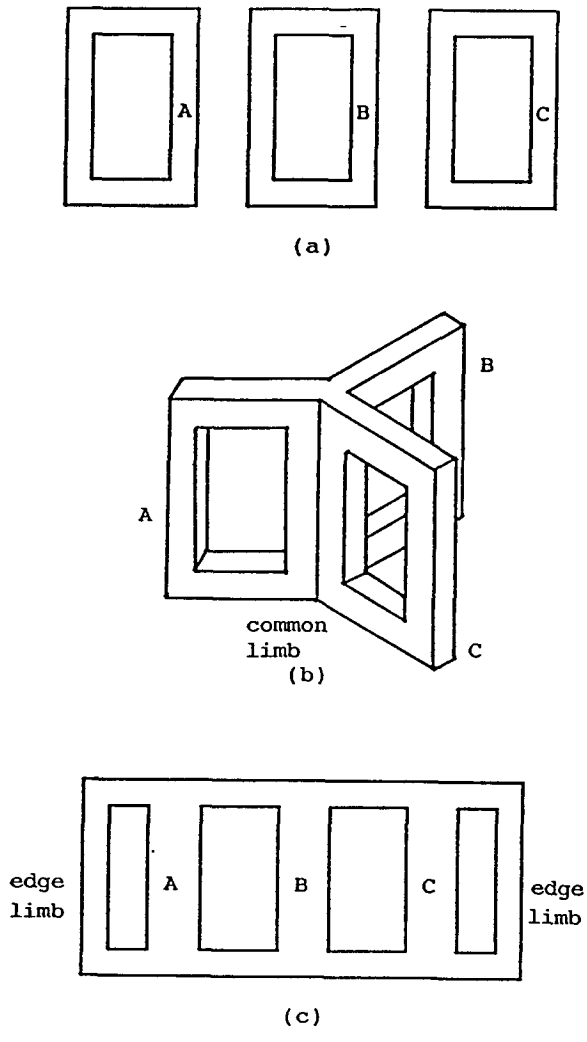

Fig. 3. Structure of three-phase transformers.

tizing current in the saturated region is not affected by the other phases. Figure 4 shows the hysteresis loop of a three-phase delta-wye connected transformer in phase A and 140V. Figure 5 shows the hysteresis loop of phase A supplied by a single-phase power source at 140V. Comparing Figs. 4 and 5, the hysteresis loop is narrower in the three-phase delta-wye connected transformer than in the independent single-phase. However, the peak values of the magnetizing currents in both hysteresis loops are nearly the same. The same results exist for different levels of excited voltages. This proves the previous assumption that a delta-wye connected magnetic circuit can be approximated by an independent circuit.

(2) For delta-delta connection:

As with a delta-delta connection of transformer banks, the secondary circular current diminishes the main flux and reduces the chance of iron core saturation. The peak magnetizing current in the saturated region indeed becomes smaller. This statement can be proved by observing experimental results.

2. The Numerical Simulation

From the above analysis of the saturation characteristics of different types of three-phase transformers, transformer banks and delta-wye connected five-limb transformers can be approximately considered as three independent magnetic circuits similar to those of single-phase transformers. The numerical method for single-phase transformers, as described in an improved model (Lin *et al.*, 1993a) using the finite difference method, can be applied to the above cases.

A power transformer is assumed to be connected to an infinite bus. By Kirchhoff's voltage law, the

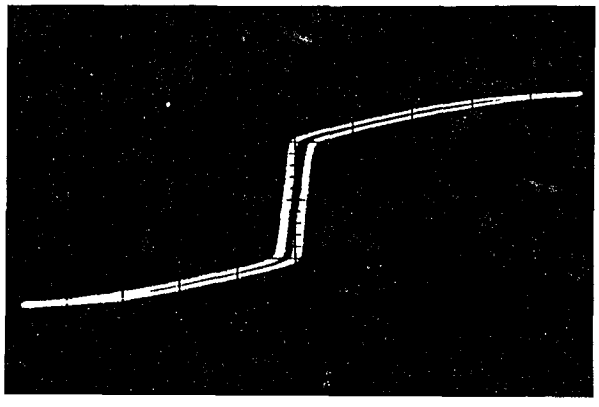

Fig. 4. Hysteresis loop of phase A in delta-wye connected five-limb three-phase transformer, measured at three-phase voltage 140V

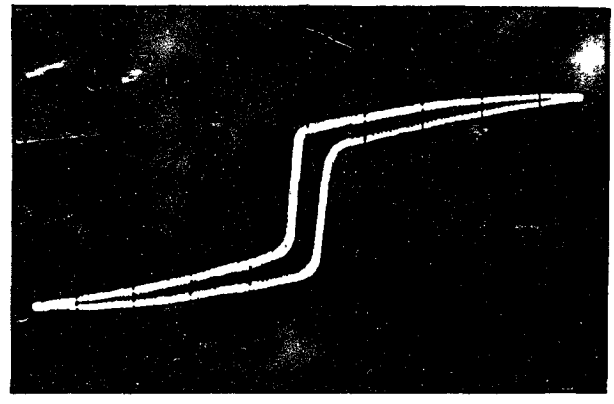

Fig. 5. Hysteresis loop of phase A in five-limb three-phase transformer, measured independently at single-phase voltage 140V.

differential equation of the primary circuit in Fig. 6 can be written as

$$e(t)=(d\lambda_1/dt)+R_1 i_1+L_1(di_1/dt), \quad (1)$$

and $e(t)=E_{max}\sin(wt+\alpha)$, (2)

where

$e(t)$ instantaneous exciting voltage,
t time measured at switching-on,
λ_1 instantaneous mutual flux linkage, in Wb.turns, in the primary winding,
i_1 instantaneous primary current,
R_1 primary circuit resistance, equal to the primary winding resistance if the source impedance is neglected,
L_1 primary circuit inductance, equal to the primary winding leakage inductance if source impedance is neglected,
E_{max} maximum voltage of $e(t)$,
w frequency of exciting voltage, in radians per second,
α switching-on angle of voltage waveform, in radians.

The differential equation of the secondary circuit in Fig. 6 can be written as:

$$d\lambda_2/dt=R_2 i_2+L_2(di_2/dt), \quad (3)$$

where

λ_2 instantaneous mutual flux linkage, in Wb.turns, in the secondary winding,
i_2 instantaneous secondary current,
R_2 secondary circuit series resistance,
L_2 secondary circuit series inductance.

When resistance increases, the load of the transformer secondary circuit drops until it is open circuited.

Equations 1 and 2 can be expressed in the finite difference form to obtain

$$e_k=E_{max}\sin(wt_k+\alpha), \quad (4)$$

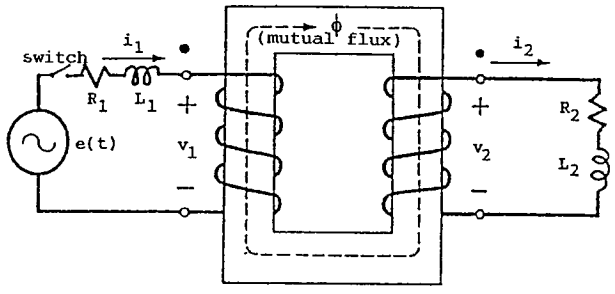

Fig. 6. Actual transformer inductive loading.

$$(\Delta\lambda_1)_k/\Delta t=e_k-R_1(i_1)_k-L_1(\Delta i_1)_k/\Delta t, \quad (5)$$

where $t_k=k\Delta t$, and k represents sampling steps in the simulation,

$$(\Delta\lambda_1)_k=(\lambda_1)_{k+1}-(\lambda_1)_k,$$

$$(\Delta i_1)_k=(i_1)_k-(i_1)_{k-1}.$$

Similarly, i_2 of Eq. 3 for different load characteristics can be written in finite difference form as

$$(i_2)_k=[(\Delta\lambda_2)_k/\Delta t-L_2\times(\Delta i_2)_k/\Delta t]/R_2, \quad (6)$$

where

$$(\Delta\lambda_2)_k=V_2/V_1\times(\Delta\lambda_1)_k,$$

where V_1 and V_2 are the primary and secondary rating voltages, respectively, and

$$(\Delta i_2)_k=(i_2)_k-(i_2)_{k-1}.$$

After $(i_2)_k$ is calculated from Eq. 6, the new $(i_1)_k$ and $(\Delta i_1)_k$ can be obtained from

$$(i_1)_k=(i_m)_k+(i_2)_k\times(V_2/V_1), \quad (7)$$

$$(\Delta i_1)_k=(i_1)_k-(i_1)_{k-1}, \quad (8)$$

where $(i_m)_k$ is the magnetizing current with respect to $(\lambda_1)_k$ as described in the Appendix.

Using Eq. 5 to Eq. 8 as one iteration routine, a new $(i_1)_k$ is obtained for the sample k. If the difference between $(i_1)_k$ from Eq. 7 and the starting value in Eq. 5 is larger than a specified tolerance, then the average of these two values is used as $(i_1)_k$ for the next iteration routine starting from Eq. 5 again. A similar process is used for $(\Delta i_1)_k$. This routine from Eq. 5 through Eq. 8 is repeated until both specified error values are achieved. Then, one simulated sample of inrush current i_1 at $t=K\Delta t$, i.e., $(i_1)_k$ is obtained from the ineration process as shown in Fig. 7. The values of $(\Delta\lambda_1)_k$ and $(i_2)_k$ can easily be calculated from both Eqs. 5 and 6 in the last iteration of k.

When $t=(k+1)\Delta t$, $(\lambda_1)_{k+1}$ can be calculated from

$$(\lambda_1)_{k+1}=(\lambda_1)_k+(\Delta\lambda_1)_k. \quad (9)$$

Then, $(i_m)_{k+1}$, corresponding to $(\lambda_1)_{k+1}$, can be calculated. For $k=k+1$, we calculate

$$(i_1)_{k+1}=(i_m)_{k+1}+(i_2)_k\times(V_2/V_1),$$

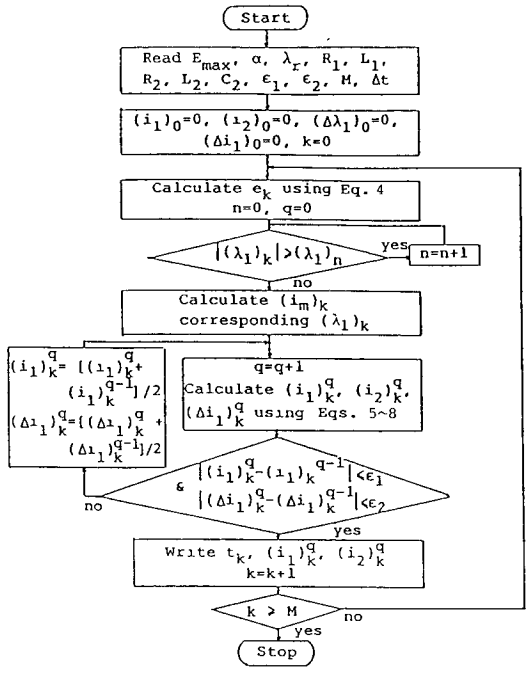

Fig. 7. Flow chart for numerical simulation.
ε_1 & ε_2: tolerance,
M: maximum simulation samples,
n: number of sampled point in hysteresis loop,
q: iteration number.

$$(\Delta i_1)_{k+1}=(i_1)_{k+1}-(i_1)_k,$$

and substitute into Eq. 5 together with e_{k+1} from Eq. 4 to obtain

$$(\Delta\lambda_1)_{k+1}/\Delta t=e_{k+1}-R_1\times(i_1)_{k+1}-L_1\times(\Delta i_1)_{k+1}/\Delta t. \quad \textbf{(10)}$$

By the same iteration procedure, $(i_1)_k$ for all k's can be obtained to get the simulation result of the magnetizing inrush current. The overall simulation procedure is shown in Fig. 7.

III. Example and Experiment

Three 3KVA 110V/220V three-phase transformers, one transformer bank, and one five-limb transformer were used for on-site measurement of the inrush current in our laboratory. The fundamental data were as follows:

	banks	five-limb
primary/secondary rating voltage	110V/220V	110V/220V
primary/secondary rating current	10A/5A	10A/5A
primary/secondary winding resistance (Ohms)	0.1/0.35	0.12/0.65
primary winding leakage inductance	0.16mH	0.19mH

The resistance and flux leakage of the secondary winding were neglected. The resistive part of load impedance (Z_2) was assumed to be very high and was regarded as an open circuit; it was fixed at 44 Ohms for all loading tests. The power factors for all different loading conditions were controlled by changing the series inductor or the parallel capacitor.

An experimental circuit for switching-on angle control in three-phase transformers is shown in Fig. 8.(Note:The switching-on angle was generally controlled via precision energization in circuit breakers.) The switches (SW) shown in Fig. 8(a) were controlled by a real-time computer, shown in detail in Fig. 8(b). The phase currents, i_a, i_b, i_c, were sampled and read into a PC-AT through a real-time measurement system. Line currents could be calculated from three phase currents. As shown in Fig. 8, RST sequence power source was supplied to the three-phase transformers, and V_{RS}' the voltage of phase A, was used as a reference for the switching-on angle in the discussion. To obtain a certain zero remanent flux, the demagnetizing process was applied before each experiment (Lin *et al.*, 1993a, 1989). The "demagnetization" process according to the following steps was applied. (1) The three-phase trans-

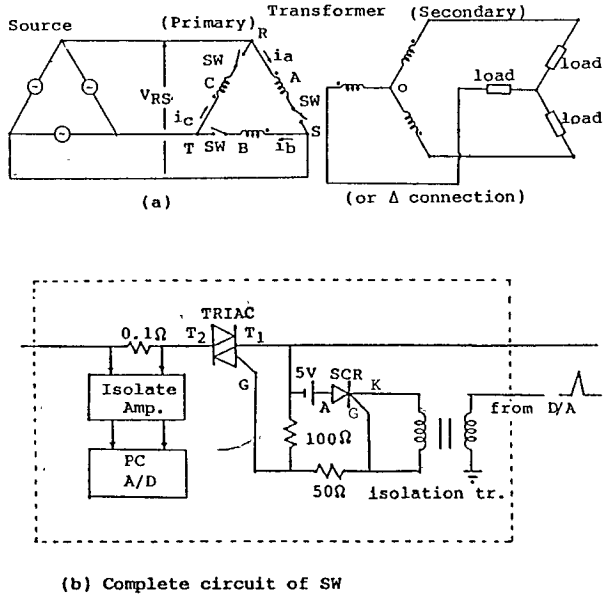

Fig. 8. Experiment circuit for switching-on angle control in three-phase transformers.

formers secondary was kept open without any load; (2) an increasing three-phase voltage was applied to the primary winding until the core reached saturation; (3) the applied three-phase voltage slowly decreased to zero; (4) the remanent flux dropped to zero.

IV. Results

The inrush currents of three-phase transformer banks and five-limb transformers were investigated. Since similar magnetic circuits existed, the results were similar. Figures and tables for five-limb transformers will be mainly presented and discussed.

1. Delta-Wye Connection

A. Switching-on Angle

When the transformer secondary was opened under zero remanent flux conditions, the inrush currents with respect to different switching-on angles were investigated. Figure 9 shows a typical inrush current measured at α=0 degrees. Table 1 shows the comparison of simulated and measured inrush currents under a switching-on angle α=0, 45, 90 degrees.

Since the possibility of flux saturation in phase A at switching-on angles of 45 degrees and 90 degrees was small, the resulting inrush currents were relatively small. Conversely, the maximum inrush current in phase A could be obtained when the switching-on angle was 0 degrees. Consequently, the inrush current in phase A decreased as the switching-on angle increases.

B. Loading Conditions

In order to investigate various relations between inrush current and loading conditions, a specified operating condition was required for comparison. The switching-on angle was kept at zero degrees, and the remanent flux linkage, λ_r, was also zero.

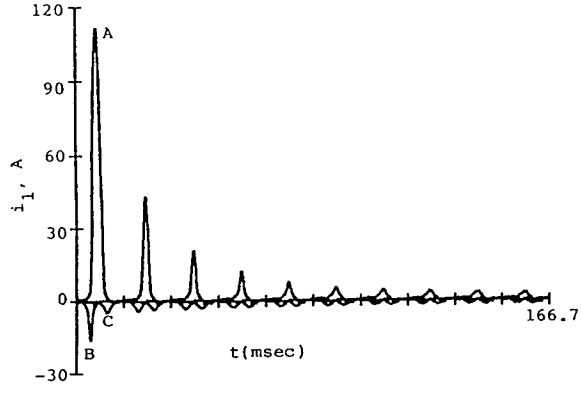

Fig. 9. Inrush current in five-limb three-phase transformers by experiment under no-load conditions, at α=0°, λ_r=0 Wb.turns.

(1) Resistive Load

A typical inrush current measured for a resistive load of R_2=44 Ohms is shown in Fig. 10. The results of comparison between the experiment data and the simulation data on peak values for 7 cycles are shown in Table 2. The magnetizing inrush current decayed in an oscillatory pattern to a normal value.

Under resistive loading conditions, the inrush current varied very sensitively with load changes. Figure 11 shows the apparent variation of peak inrush currents with load resistances in the transformer secondary. The main flux interacted with the reverse linkage flux resulting from secondary currents. The larger the secondary currents were the smaller was the resulting inrush current since there was less chance of causing iron core saturation.

(2) Inductive Load

Under inductive loading conditions, the inrush current was sensitive to load power factors. The experimental results and the simulation results are compared in Table 3 on their peak values for 7 cycles under conditions of a 0.8 lagging power factor with Z_2=44 Ohms. Figure 12 shows the variations of peak inrush currents to load power factors. The main flux strongly interacted with the real part of reverse linkage

Table 1. Effect of Switching-on Angle α on Peak Inrush Current in Five-Limb Three-Phase Transformers. S*: simulation result, E+: experiment results

α	Phase	Cycle (A)	1	2	3	4	5	6	7
	A	S*	114.3	42.0	19.2	11.5	7.3	5.5	4.5
		E+	110.6	40.1	18.9	11.0	7.1	5.3	4.3
0	B	S*	-14.5	-4.0	-2.8	-2.5	-2.2	-1.9	-1.8
		E+	-13.9	-3.8	-2.7	-2.3	-2.1	-1.9	-1.7
	C	S*	-9.0	-3.7	-2.9	-2.5	-2.2	-2.0	-1.9
		E+	-8.5	-3.5	-2.8	-2.5	-2.1	-2.0	-1.8
	A	S*	55.5	16.5	9.2	6.4	5.0	4.3	3.8
		E+	54.1	15.9	9.0	6.1	4.9	4.2	3.7
45	B	S*	4.1	2.7	2.5	2.4	2.3	2.2	2.1
		E+	3.9	2.5	2.5	2 4	2.3	2 2	2.1
	C	S*	-91.4	-32.0	-10.1	-5.2	-3.8	-3.3	-2.6
		E+	-89.1	-30.5	-9.6	-5.0	-3.7	-3.2	-2.5
	A	S*	1.4	1.3	1.3	1.3	1.3	1.3	1.3
		E+	1.4	1.4	1.4	1.4	1.4	1.4	1.4
90	B	S*	78.5	30.1	14.0	7.8	5.6	4.8	4.1
		E+	76.1	28.7	13.1	7.5	5.5	4.8	4.0
	C	S*	-74.1	-16 1	-5.3	-4.0	-3.3	-2.7	-2 4
		E+	-72.4	-15.7	-5.1	-3.9	-3.2	-2.6	-2.4

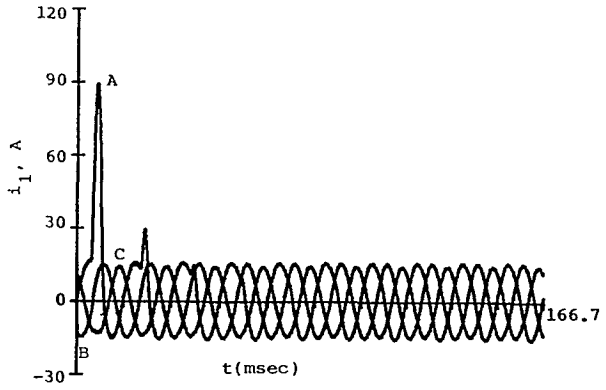

Fig. 10. Inrush current in five-limb three-phase transformers by experiment under resistive load conditions, at α=0°, λ_r=0 Wb.turns, R_2=44 Ohm.

Table 2. Comparison of Simulation Data (S*) and Experiment Data (E+) in Five-Limb Three-Phase Transformers, at R_2=44 Ohm

Phase	Cycle	1	2	3	4	5	6	7
A	S*	88.0	33.2	17.1	16.2	16.1	16.0	16.0
	E+	87.3	32.1	16.7	15.9	15.9	15.9	15.9
B	S*	-15.2	-15.1	-15.1	-15.0	-15.0	-15.0	-15.0
	E+	-15.0	-15.0	-14.9	-14.9	-14.9	-14.9	-14.9
C	S*	-14.6	-14.5	-14.5	-14.4	-14.4	-14.3	-14.3
	E+	-14.5	-14.4	-14.4	-14.4	-14.3	-14.3	-14.3

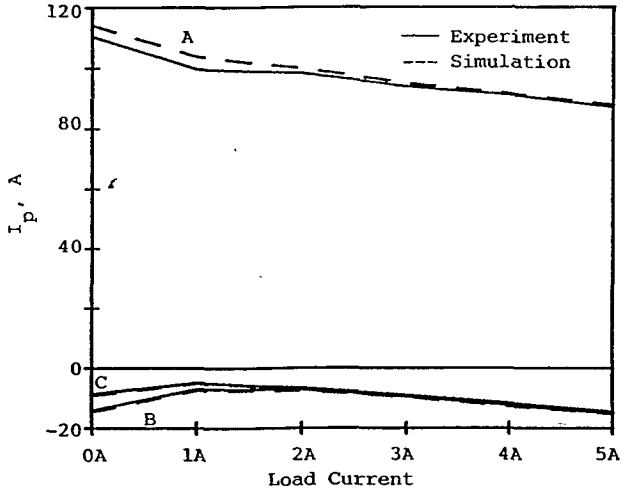

Fig. 11. Effect of resistive load on peak inrush current in five-limb three-phase transformers, at α=0°, λ_r=0 Wb.turns.

flux resulting from secondary currents. A higher power factor could result in a smaller peak inrush current since the chance of iron core saturation decreased.

(3) Capacitive Load

Table 3. Comparison of Simulation Result (S*) and Experiment Result (E+) in Five-Limb Three-Phase Transformers, at α=0°, λ_r=0 Wb.turns, pf=0.8 lagging, Z_2=44 Ohm

Phase	Cycle	1	2	3	4	5	6	7
A	S*	93.2	45.0	28.1	21.0	17.6	17.1	17.0
	E+	91.0	42.7	27.0	20.5	17.3	17.1	17.0
B	S*	-15.5	-15.3	-15.3	-15.2	-15.2	-15.2	-15.1
	E+	-15.2	-15.2	-15.1	-15.1	-15.1	-15 1	-15.1
C	S*	-15.1	-15.0	-15.0	-15.0	-14.9	-14.9	-14.9
	E+	-14.5	-14.5	-14.4	-14.4	-14.4	-14.4	-14.3

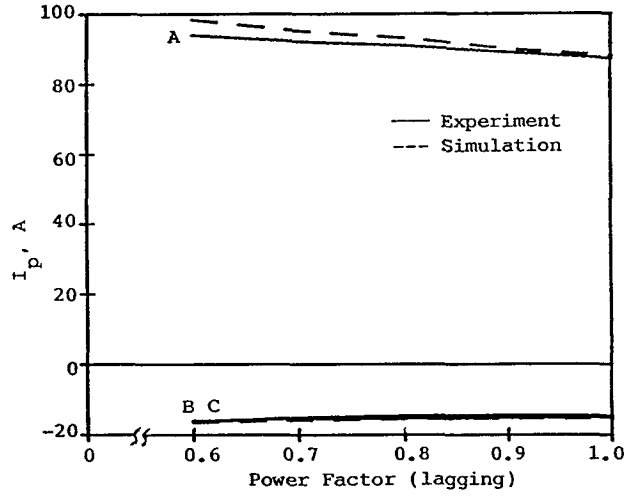

Fig. 12. Effect of inductive load on peak inrush current in five-limb three-phase transformers, at α=0°, λ_r=0 Wb.turns.

Under capacitive loading conditions, the inrush current also had a close relationship with load power factors. The experimental results and the simulation results are compared in Table 4 on their peak values for 7 cycles. Figure 13 shows the variations of peak inrush currents to load power factors. When the power factor was close to 1.0, the peak inrush current was small. The reason for this effect was similar to that

Table 4. Comparison of Simulation Result (S*) and Experiment Result (E+) in Five-Limb Three-Phase Transformers, at α=0°, λ_r=0 Wb.turns, pf=0.8 leading, Z_2=44 Ohm

Phase	Cycle	1	2	3	4	5	6	7
A	S*	92.8	25.0	17.3	17.3	17.2	17.2	17.1
	E+	89.7	23.7	16.9	16.9	16.9	16.8	16.8
B	S*	-16.6	-16.5	-16.5	-16.4	-16.4	-16.3	-16.3
	E+	-17.4	-16.7	-16.3	-16.3	-16.2	-16.2	-16.1
C	S*	-15.3	-15.3	-15.2	-15.2	-15.2	-15.1	-15.1
	E+	-15.3	-15.2	-15.2	-15.2	-15.1	-15.1	-15.1

for an inductive load.

C. Power Source Voltage

In Fig. 14, the simulating results show the influence of the applied voltage in the transformer primary on the resulting inrush current. The approximately linear relationship of the applied voltage and the peak inrush current in phase A is an important and impressive phenomenon in this study.

2. Delta-Delta Connection

When the secondary windings were delta-connected, a circular current existed. The magnitude of this circular current was sensitive to the load unbalance. For a more circular current, more main flux is diminished by its reverse linkage flux. Therefore, a smaller inrush current was expected.

The hysteresis loops with delta-delta and delta-wye connections are shown in Figs. 2 and 1. Comparing Fig. 2 with Fig. 1, the peak value with a delta-delta connection is obviously smaller than that with a delta-wye connection. Figure 15 shows the comparison of inrush currents both in delta-delta and delta-wye connections under various resistive loads. The corresponding results are listed in Table 5. Observing Fig. 15 and Table 5, it is proved that a delta-delta connection leads to a smaller inrush current than does a delta-wye connection.

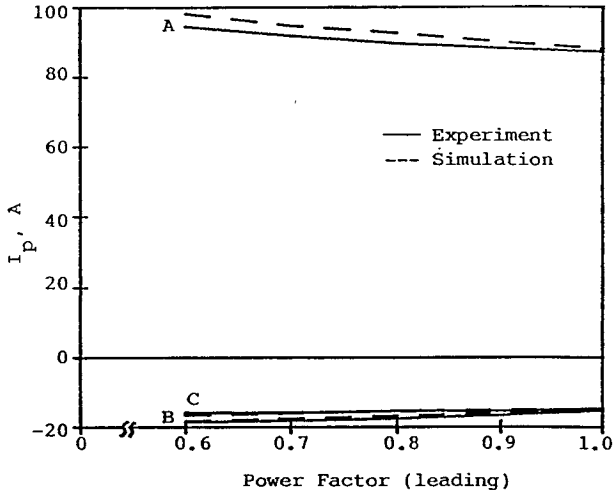

Fig. 13. Effect of capacitive load on peak inrush current in five-limb three-phase transformers, at α=0°, λ_r=0 Wb.turns.

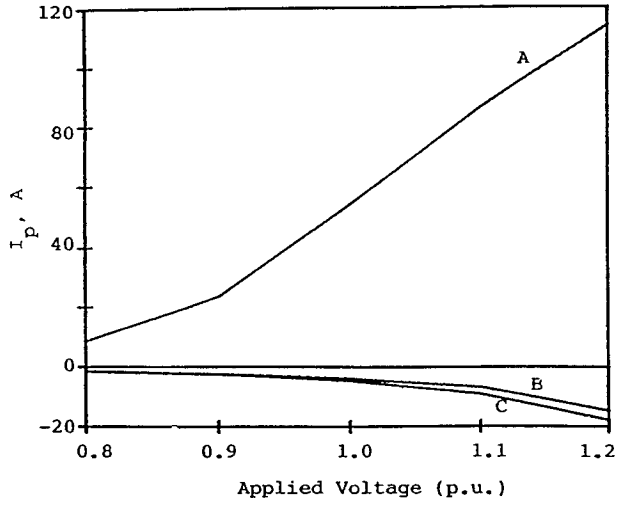

Fig. 14. Effect of voltage on peak inrush current in three-phase transformer banks at α=0°, λ_r=0 Wb.turns.

V. Conclusions

Table 5. Comparison of Δ-Δ and Δ-Y Peak Inrush Currents in Five-Limb Three-Phase Transformers.

R_2 (I_2)	Phase	I_p(A) Δ-Y	I_p(A) Δ-Δ
∞Ω (0A)	A	110.6	93.6
	B	-13.9	-19.2
	C	-8.5	-19.3
88Ω (2 5A)	A	97.4	83.0
	B	-8.1	-9.0
	C	-7.7	-21.8
44Ω (5A)	A	87.3	78.1
	B	-15.0	-14.9
	C	-14.5	-27.1

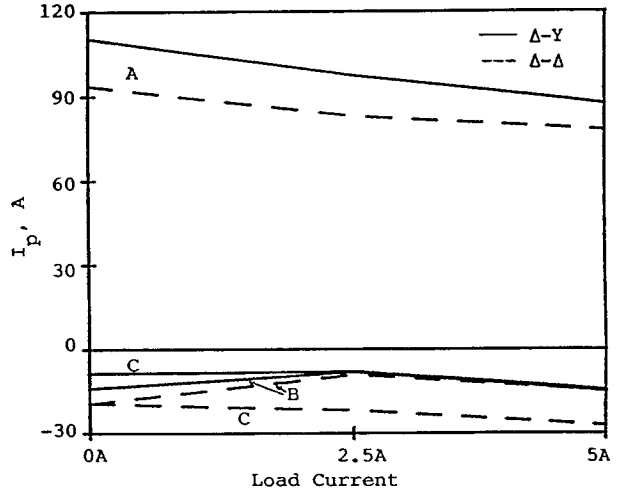

Fig. 15. Comparison of delta-delta and delta-wye peak inrush currents in five-limb three-phase transformers.

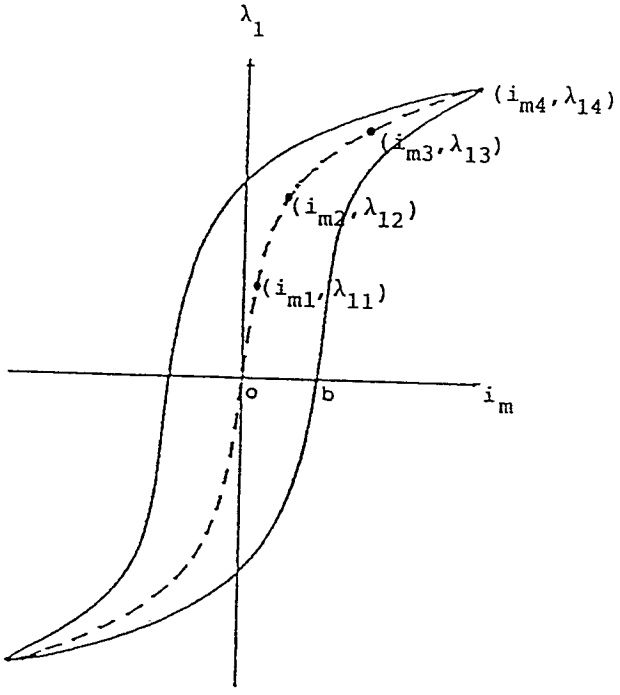

Fig. A-1. Simple hysteresis curve.

This paper has demonstrated a simple and effective method, extended from the method for single-phase transformers (Lin *et al.*, 1993a), for predicting the magnetizing inrush current in three-phase transformers. Various investigations have been described relating to transformer loading conditions, switching-on angles, remanent flux, and winding connections of three-phase transformers of different types.

The data used in this paper were easy to obtain, as compared to other developed methods which require many parameters and complicated processes. These results prove the validity of the proposed method for practical application. For various loading conditions, the proposed method can still accurately predict the transient inrush current.

Consequently, more detailed knowledge of the inrush current in three-phase transformers has been gained in this study. By using the proposed method, preparation time and field experiment work can be reduced. The proposed method can be applied to investigate problems caused by inrush currents in three-phase transformers.

Acknowledgments

This work was supported by the National Science Council under research project NSC80-0404-E006-04.

Appendix

The mathematical expression of the i_m–λ_1 hysteresis cure.

The mathematical expression of the i_m–λ_1 hysteresis curve (Lin *et al.*, 1989) in Fig. A-1 is

$$i_m = i_{mn} + s_n(\lambda_1 - \lambda_{1n}) + ob \times \sin(wt+\alpha), \text{ for } \lambda_1 \geq 0,$$

$$= -[i_{mn} + s_n(-\lambda_1 - \lambda_{1n})] + ob \times \sin(wt+\alpha), \text{ for } \lambda_1 < 0, \quad \textbf{(A-1)}$$

where $\lambda_{1(n-1)} < |\lambda_1| \leq \lambda_n$,

i_m instantaneous magnetizing current,
λ_1 instantaneous mutual flux linkage, in Wb.turns,
s slope of the corresponding line sections,
ob the maximum distance between the mid-point locus and the periphery of the hysteresis loop,
and n=1, 2, 3, 4. The accuracy of the above mathematical model can be improved by increasing n, the number of line sections.

References

Badawy, E. H. and R. D. Youssef (1983) Representation of transformer saturation. *Electric Power Systems Research*, **6**(4), 301-304.

Hwang, M. S., W. M. Grady, and H. W. Sanders (1987) Distribution transformer winding losses due to nonsinusoidal Currents. *IEEE Trans. on PWRD*, **2**(1), 140-146.

Hwang, M. D., W. M. Grady, and H. W. Sanders (1988) Calculation of winding temperatures in distribution transformers subjected to harmonic currents. *IEEE Trans. on PWRD*, **3**(3), 1074-1079.

Keyhani, A. and S. M. Miri (1988) Nonlinear modeling of magnetic saturation and hysteresis in an electromagnetic device. *Electric Power Systems Research*, **15**(1), 15-24.

Lin, C. E., J. B. Wei, C. L. Huang, and C. J. Huang (1989) A new model for transformer saturation characteristics by including hysteresis loops. *IEEE Trans. on MAG*, **25**(3), 2706-2712.

Lin, C. E., C. L. Cheng, C. L. Huang, and J. C. Yeh (1993a) Investigation of magnetizing inrush current in transformers Part I - Numerical simulation. *IEEE Trans. on PWRD*, **8**(1), 246-254.

Lin, C. E , C. L. Cheng, C. L. Huang, and J. C. Yeh (1993b) Investigation of magnetizing inrush current in transformers Part II - harmonic analysis. *IEEE Trans. on PWRD*, **8**(1), 255-263.

Macfadyen, W. K., R. R. S. Simpson, R. D. Slater, and E. S. Wood (1973) Method of predicting transient current patterns in transformers. *IEE Proc.*, **120**(11), 1393-1396.

Nakra, H. L. and T. H. Barton (1974) Three phase transformer transients. *IEEE Trans. on PAS*, **93**(6), 1810-1819.

Prusty, S. and M. V. S. Rao (1984) A novel approach for predetermination of magnetization characteristics of transformers including hysteresis. *IEEE Trans. on MAG*, **20**(4), 607-612.

Rahman, M. A. and A. Gangopadhyay (1986) Digital simulation of magnetizing inrush currents in three-phase transformers. *IEEE Trans. on PWRD*, **1**(4), 235-242.

Rivas, J., J. M. Zamarro, E. Martin, and C. Pereira (1981) Simple approximation for magnetization curves and hysteresis loops. *IEEE Trans. on MAG*, **17**(4), 1498-1502.

Swift, G. W. (1971) Power transformer core behaviour under transient condition. *IEEE Trans. on PAS*, **90**(5), 2206-2210.

Yacamini, R. and A. Abu Nasser (1986) The calculation of inrush current in three-phase transformers. *IEE Proc., Pt. B*, **133**(1), 31-40.

三相變壓器組與外鐵式變壓器暫態電流之數值模式

黃慶連　葉進純　林清一　鄭健隆

成功大學電機工程研究所

摘　要

當三相變壓器起始激能時，由於鐵心的磁通過飽和的現象，將造成過電流之暫態現象，它會引起保護電驛系統的誤動作，所以，對三相變壓器之激磁暫態電流的特性，值得去加以研究，因此，若能提出一數學模式來準確地加以預測暫態電流，則對系統的操作與保護會很有幫助。本文乃延伸自單相變壓器的方法，提出一簡單的數學模式，來探討三相變壓器過電流之暫態現象。對於三相變壓器不同的結構，如繞組的連接方式及負載狀況，均有詳加討論。最後，經比較測量值與模擬值，來驗證所提方法可以很簡單且有效地應用於三相變壓器組與外鐵式變壓器。